Submitted to the IMECE Haptics Symposium, Dallas, Texas, 1997

Temporal Bandwidth Requirements for Tactile Shape Displays

William J. Peine, Parris S. Wellman and Robert D. Howe

Harvard University
Division of Engineering and Applied Sciences
Pierce Hall, 29 Oxford Street
Cambridge, Massachusetts 02138 U.S.A.

TEL (617) 496-9098 FAX (617) 495-9837
EMAIL: peine@hrl.harvard.edu

Abstract:

Haptic interfaces that include tactile shape displays must correlate small-scale shape information with finger position. High temporal bandwidth of the display actuators is required to provide realistic sensation during rapid finger motions. To characterize finger speeds during surgical palpation, we performed an experiment where subjects used the tip of the index finger to search for 4 mm lumps embedded in flat rubber models. The models were 15 to 25 mm thick soft silicone rubber with mechanical characteristics approximating lung or breast tissue. Average fingertip speed while in contact with the rubber was approximately 38±16 mm/s (mean ± standard deviation), and average maximum speed was 90±31 mm/s. While moving between contact intervals, the average fingertip speed was approximately 76±18 mm/s, and average maximum speed was 146±37 mm/s. There were no significant speed differences between experienced surgeons and subjects who had no medical training. The results indicate that a 30 Hz bandwidth is necessary for shape displays used in haptic interfaces for lump localization in surgery. A shape display design meeting this specification is also presented.

1. Motivation

Tactile displays capable of creating small-scale shapes on the fingerpad have important applications in feedback systems for surgical instrument [Cohn, Lam, and Fearing 1992; Howe et al. 1995; Fischer, Neisius, and Trapp 1995], tele-operated robots [Kontarinis et al. 1995], and virtual reality interfaces [Hasser and Weisenberger 1993]. In these systems, a master manipulator or mechanical linkage provides overall motion and force information while a shape display provides contact information on the fingerpad. The display approximates the remote or virtual object's shape by raising or lowering an array of individually actuated pins. The design and construction of these displays is a tremendous challenge due to the numerous design requirements. Naturally, objects feel more realistic as the spatial density of the pins increases. However, decreasing pin to pin spacing is difficult because actuator limitations. The pins need 2 to 3 mm of pin displacement 1 to 2 N of force to impose skin deflections during large loads. Additionally, the display must also be small, light, and have a minimum number of cables so that it can be mounted on a surgical instrument or robot manipulator.

In order for a haptic feedback system to provide realistic sensations of a remote or virtual object, it is important to correlate the tactile shape information with overall finger motions and forces. This coupling of kinesthetic and cutaneous sensations allows operators to gain large-scale information about an object by scanning their fingers over its surfaces. For this to feel correct, it is then important that tactile features on the object's surface stay fixed relative to the object's coordinate frame. Therefore, another important design consideration for the display is high temporal bandwidth of the pins. The faster the finger is scanned across the object, the faster the pins must move in order to create the sensation of the tactile feature moving across the fingerpad. Ideally, haptic interfaces allow natural finger motions and speeds for exploration. Temporal bandwidth design specifications could thus be set to match maximum finger speeds during natural haptic exploration.

An especially promising application for haptic feedback is remote palpation instruments for minimally invasive surgery. In this type of surgical technique, access to the surgical site is limited to a few small incisions so the surgeon is deprived of the ability to directly touch or palpate the tissue. This is problematic when locating objects embedded in a surrounding tissue. Finding lung tumors in thoracoscopic resections, for example, is tedious and time consuming without tactile feedback. The tumor's existence is established by pre-operative imaging, but its precise location varies as the lung deflates during surgery [Mack et al. 1993]. Vision alone is often inadequate to locate the tumor. It could, however, be quickly localized by feeling for the hard lump using a surgical instrument with a tactile sensor on the probe tip measuring the pressure distribution across the contact with the tissue, and a tactile display recreating this pressure pattern on the surgeon's finger. The probing motions used with the instrument would be similar to natural palpation using the index finger alone.

In order to determine pin bandwidth requirements of a shape display used in a remote palpation instrument, it is important to characterize typical finger speeds used by surgeons during palpation. In this paper we present an experiment designed to determine typical finger speeds used when localizing hard lumps in a soft material using the index finger. We also present a shape display design which focuses on providing pins with high temporal bandwidth.

2. Finger Speed in Single Digit Palpation

In the experiment described here, we created rubber models with embedded ball bearings to emulate soft tissues with tumors. As subjects palpated these models to locate the hard lumps, we measured finger tip position and applied force. To determine if the gross mechanical properties of the tissue has a major effect on finger speed, we used three different types of rubber model, varying the thickness of the rubber and adding a stiffer skin to the surface. The measured finger locations were analyzed to determine average and maximum speed for each of these model types. To determine if medical training influenced palpation technique, the subjects included surgeons as well as individuals with no medical training. The experimental design draws upon the fundamental work of

Pennypacker and colleagues, which is unique in its systematic approach to the study of palpation [Pennypacker and Iwata 1990]. These studies quantified the main psychophysical parameters for lump detection in breast self-examination, including the roles of lump size, stiffness, depth, background nodularity, search pattern, and training.

2.1 Experimental Methods

We created rubber models with mechanical characteristics similar to tissues commonly palpated during surgery. They were constructed by filling a plastic petri dish (88 mm diameter, 15 mm deep) with a soft two-part silicone rubber (General Electric RTV6166, Young's modulus $\cong$ 3 kPa). To simulate tumors or hard lumps in the rubber models, 4 mm steel ball bearings were glued to the bottom of each dish before the rubber was added. Pilot studies indicated that 4 mm was large enough that subjects could locate every ball and small enough that it required thorough searching to find them. This accords with the results of Adams et al. [1976] who found that the ability to detect 4 mm lumps in more complex simulated silicone breasts averaged over 90 percent. The number of ball bearings in the models was varied between two and four to ensure that subjects searched the entire model carefully.

To determine if alterations to the thickness and stiffness of the model caused large variations in palpation strategies, we modified the "reference" version described above (15 mm thick homogeneous rubber) in two ways. The first "thicker" variation consisted of a homogeneous 25 mm layer of the same rubber. The second "skinned" variation added a 1 mm thick skin of stiffer rubber (General Electric RTV108, Young's modulus $\cong$ 600 kPa) on top of the softer 15 mm layer. All of the rubber models were powdered with talc to limit the stickiness of the surface of the rubber; however, significant friction was still present between the rubber and human finger tip.

The experimental apparatus is shown in Figure 1. For each trial, the experimenter placed a model on top of a strain-gauge force sensor which measured the normal forces applied to the model by the subject's finger. An optical position sensing device (models OT-3210 and OT-300l, On-Trak Photonics Inc., Lake Forest, CA, with a 50 mm lens)

located 70 cm above the model measured the position of a light emitting diode (LED) glued to the subject's finger nail. This system measured the x and y coordinates of the finger tip within the plane parallel to the top surface of the model. The output signals from the force and position sensors were hardware filtered using four-pole low-pass filters with corner frequencies at 20 Hz. These signals were digitized to 12 bits at a sample rate of 100 Hz. The peak-to-peak noise amplitude of the force sensor and position sensor was approximately 0.013 N and 0.05 mm respectively. In software, the measured signals were filtered with a six-pole low-pass filter with a corner frequency of 15 Hz. Pilot studies indicated 95 percent of the measured signal power was below 3 Hz. Velocities in the x and y directions were found by performing numerical differencing of adjacent samples of the filtered position data. Finger speed was then calculated by finding the magnitude of the velocity vector.

A total of 12 subjects, naive to the purposes of the study, voluntarily participated in the experiments (8 male, 4 female). To determine the effect of professional experience on palpation technique, we divided the subjects into two groups: 'experts' and 'novices.' The experts consisted of five surgeons (ages 35-45, mean 39) with an average of 13 years surgical experience, and the novices included seven individuals with no medical training (ages 19-54, mean 27).

Each subject completed 18 trials. A trial consisted of locating all of the lumps in one of the models. A partial Latin squares presentation order based on model type and number of lumps was used to eliminate learning effects. For each trial, the subject was instructed to wait for a beep from the data acquisition computer and then insert his or her dominant hand through a 14 cm hole in an opaque screen, and probe the model with the index finger. When a lump was detected, the subject centered the finger over the lump and pressed a button with the other hand. The subject then continued searching the model until they were satisfied they had found all the lumps. After finishing the search, the subject removed his or her hand from the screen and told the experimenter the trial was completed. To discourage exceeding the force sensor range, a buzzer sounded when

forces were above an acceptable level (≅ 15 N), a realistic limit for palpation of tissues in vivo.

2.2 Results

The position and force data collected during the experiment revealed that all of the subjects used the same basic palpation procedure when searching for a lump. This consisted of pressing the finger into the model, making a small circular motion around the contact point, retracting out of contact with the model, then moving to a new contact location. This simple motion was repeated many times, with the contact points following a systematic search pattern. All of the subjects consistently used one of three patterns: six subjects used a spiral pattern starting with the outside edge and circling in to the center; five used a vertical strip pattern with a series of lines scanned from top to bottom; and one used a spoked wheel pattern with lines radiating from the center.

Using the force data, each trial was segmented into a series of contact intervals. Figure 2 shows the force record from part of a typical trial on a thicker model containing three lumps. This same data is used in Figures 3 and 4. The force record consists of a series of peaks separated by periods of no force. Each interval corresponds to one of the probing motions described above. The bottom trace in the plot shows when the subject pressed the button, indicating a lump had been located. The trial was segmented using a threshold of 1 N to find the starting and ending points for each contact interval. A plot of the segmented x and y position data along with the location of the lumps is shown in Figure 3. The circular motions that occur when the finger is pressed against the model can be distinguished from the translation used when moving to a new contact point.

For each contact interval of each trial, we then calculated the mean, standard deviation, and maximum of the speed during the interval. Figure 4 shows these values for all of the intervals in this typical trial. The average speed during the intervals when a lump was located is much slower because subjects were instructed to center their finger over the lump while pressing the button.

Once all of the trials for one subject had been segmented, we concatenated intervals of the same model type into groups. The average speed for each group was calculated by finding the mean of the group. The average maximum speed for the group was found by taking the mean of all the maxima measured during each interval in the group. Similarly, we found the mean and average maximum speed used between contact intervals.

The mean and maximum speeds calculated for the three model types and for non-contact motion are shown in Table 1. The skinned models had a mean slightly lower than the reference models, and the thicker models had a mean slightly higher. In contrast, the mean speeds used between contact intervals were much higher. The maximum speeds followed similar trends, with the exception that the reference model had the lowest average maximum. Using matched pair *t* tests, we compared the reference model with the two variations to determine if the differences in the means were significant. The results are shown in Table 2. For the thicker models, we found a significant difference for the average and maximum speed. For the skinned models, we found a significant difference in the average speed, but not for the maximum speed. Although we found some significance in these variations, the means are within 15 percent of the reference model. When contrasting these speeds to the non-contact speeds used between contact intervals, however, the variations are strongly significant.

Rubber Model Type	*Mean Average Speed, mm/s*	*Standard Deviation*	*Mean Maximum Speed, mm/s*	*Standard Deviation*
Contact Motion:				
Reference (15 mm)	39.24	18.06	83.95	31.10
Thicker (25 mm)	42.15	18.34	97.77	36.12
Skinned (15 mm with skin)	33.71	13.10	87.75	27.05
Non-contact Motion:				
All model types	76.12	18.62	146.49	36.91

Table 1. Mean and standard deviation for average and maximum speeds used for the three model types and for non-contact motion.

Rubber Model Type	*Average Speed*		*Maximum Speed*	
	t_{11}	p	t_{11}	p
Contact Motion:				
Thicker (25 mm)	2.782	0.018	5.185	0.002
Skinned (15 mm with skin)	3.161	0.009	0.844	0.390
Non-contact motion:				
All model types	6.036	0.001	6.016	0.001

Table 2. Results from matched pair t tests comparing speeds used for the reference model to the speeds used for the other 2 model types and for non-contact motion.

The last factor we tested was level of expertise. We found no significant difference between experts and novices. (Average speed: $t_{5.7} = 0.022$, $p > 0.9$; Maximum speed: $t_{5.7} = 0.603$, $p > 0.5$)

Figure 8 shows cumulative distribution functions for the mean and maximum speeds used with each of the three model types and for non-contact motion. These curves allow bandwidth requirements for the tactile shape display to be specified. As an example, consider a shape display with actuated pins spaced 2 mm apart. The maximum spatial frequency the display can create (i.e. the Nyquist limit, with pins alternating up and down) is then 0.25 cycles/mm. From the cumulative distributions, finger speeds for 90 percent of the population tested would peak near 120 mm/s, depending on "tissue characteristics." If the maximum spatial frequency is scanned across the display at this rate, each pin must travel up and in 33.3 msec. This means the required temporal bandwidth for each pin be at least 30 Hz.

3. Shape Display Design

Designing a shape display with a temporal bandwidth of 30 Hz is a formidable challenge. In previous work, we constructed 2D arrays, but this was difficult because of space limitations and the resulting pin speeds were too slow. We opted to decrease the number of pins and concentrate on developing fast actuators. The design reported here

uses a single line of 10 actuated pins spaced 2.0 mm on center. This gives an overall coverage of 20 mm, which is adequate to span the length of most fingers. A single line was chosen because of the reduced complexity and because it is possible for users to sweep the display across a surface in order to determine 2D shape.

As in previous designs, we chose nickel-titanium strain memory alloy (SMA) to actuate each pin because of its high force density, compact size and ability to produce large forces and displacements through the strain memory effect. Electric current is used to heat the wires, which shorten as they undergo a phase transformation from the heating. Because the frequency response of SMA depends directly on how well it is cooled, we have used a recirculating water bath in which the wires are immersed. Two thin (76.2 micron) wires are used to actuate each pin instead of one thicker wire in order to maximize the surface area available for heat transfer. We use SMA with a transition temperature of 90° C in order to maximize cooling.

The wires are arranged in a V shape with the pin at the apex of the V. Figure 6 shows a top and side view of the display. This configuration provides a mechanical advantage which amplifies the displacement of the wires and is

$$\frac{\Delta y}{\Delta L} = \frac{1}{\sin(\theta)} \qquad (1)$$

where Δy is the change in height of the pin, ΔL is the change in length of the wire and θ is the angle the wire makes with the circuit board (see figure 6). At 4% strain in the wires, the pins provide 3.5 mm of displacement. Maximum forces applied to the pin should be limited to prevent permanent deformation of the wires. Taking into consideration the mechanical layout and yield strength specified by the manufacture, this maximum force is approximately 1 N per pin. However, in our tests application of over twice this value has not produced any observable permanent deformation.

The display itself is a multi-layer construction with all electrical components mounted on one circuit board. The ends of each SMA wire are copper plated and soldered into the board to provide mechanical restraint and electrical connection. The overall size of the display is 68 mm wide, 35.5 deep, and 70 mm high, making it compact enough to mount

on a surgical instrument or a telemanipulator master. A rubber membrane is mounted on top of the display to act as a spring return for each pin and also to seal the display.

We have demonstrated that the display produces 2.5 mm displacements at 30 Hertz while supporting a 60 gram load on each pin. Figure 7 shows the open-loop response of a representative pin. We have incorporated optical feedback using an infrared LED and a photo-darlington transistor to sense the position of the pin. Work to include position feedback into a control algorithm is underway. The controller will be used to keep the wire at the minimum temperature required to begin phase transformation and shortening of the wires. This will improve the performance of the display by minimizing the time required to begin motion and will eliminate the effect seen in figure 7 where the wires gradually heat up during the first few cycles. Closed loop feedback will also help to eliminate the effect of changes in cooling.

4. Discussion

Haptic interfaces that include tactile displays to create small-scale shape on the fingerpad must correlate contact information with overall finger motions and forces. This is important so that small-scale tactile features on an object feel fixed relative to the object. People scan their fingers over the feature to learn large-scale information. This also provides a time varying stimulus to the mechanoreceptors in the skin. If the tactile display is to keep up with the finger motions, the bandwidth of the display must be sufficiently high.

It is therefore important to understand how the fingers are used to haptically explore an object. We have investigated a localization task in this paper. This is only one type of palpation procedure. Varying hand and finger mobility constraints or object properties will change palpation technique. For example, it was observed in the experiment that subjects did not slide over the surface of the model during a contact interval. The lateral motions the subjects used did not create tangential forces that exceeded the surface friction of the models; these frictional conditions are realistic for a subset of surgical procedures. Under these conditions it may be advantageous to avoid slips because sliding

causes irregular shear forces on the finger which can mask the sensation of the lump [Lederman 1978]. In addition, remaining in contact with a fixed point on the surface may make it easier to correlate kinesthetic and tactile information. In some surgical procedures, however, the tissue of interest may present a relatively regular and slippery surface where smooth sliding is possible. Further experiments are planned to determine palpation strategies and finger velocities under these conditions.

These results indicate that in a simple palpation task the finger speeds used by surgeons are not significantly different from speeds used by individuals with no medical training. Harris et al. [1994] found no significant differences in psychomotor skills of surgeons compared with other medical specialists. The similarity of speed across training level also supports the conjecture that speeds are optimized for the limitations of the human sensory-motor system. It should be noted that the experiment used a straightforward detection task that largely involved motor and perceptual faculties. Differences between surgeons and novices are more likely to be evident in complex tasks that require higher level functions such as discrimination and diagnosis.

The experiment described here is in no way a definitive study. It is only the beginning of ongoing pursuit to understand more about palpation. There are many other issues to be determined concerning how and why people haptically explore an object in a certain way. This will provide insight into the workings of the human sense of touch as well as determine significant design specifications, such as temporal bandwidth, for tactile displays.

Acknowledgments

The authors would like to thank Cindy Barlow for assistance with the experiments and Roberta Klatzky and Susan Lederman for helpful discussions. This work was supported by the Whitaker Foundation under the Biomedical Engineering Research Grants Program and the Office of Naval Research University Research Initiative Program under grant no. N00014-92-J-1887.

References

Adams, C. K., Hall, C., Pennypacker, H. S., Goldstein, MK, Hench, LL, Madden, MC, Stein, GH, and Catania, AC, 1976. "Lump detection in simulated human breasts," *Perception & Psychophysics*, **20**(3), pp. 163-167, 1976.

Cohn, M. B., Lam, M., and Fearing, R.S., "Tactile Feedback for Teleoperation." *Proc. Telemanipulator Technology,* H. Das, Editor, Boston, Proc. SPIE **1833**, pp. 240-254, 1992.

Fischer, H., Neisius, B., and Trapp, R., "Tactile Feedback for Endoscopic Surgery," in K. Morgan, R. Satava, H. Sieburg, R. Mattheus and J. Christensen, Eds., *Interactive Technology and the New Paradigm for Healthcare*, IOS Press, Amsterdam, pp. 114-117, 1995.

Harris, C. J., Herbert, M., and Steele, R. J. C., "Psychomotor Skills of Surgical Trainees Compared with Those of Different Medical Specialists," *British Journal of Surgery*, **81**, pp. 382-383, 1994.

Hasser, C. and Weisenberger, J. M., "Preliminary Evaluation of a Shape-Memory Alloy Tactile Feedback Display" in *Advances in Robotics, Mechatronics, and Haptic Interfaces*, DSC-vol. 49,H. Kazerooni, J. E. Colgate, and B. D. Adelstein, eds., American Society of Mechanical Engineers Winter Annual Meeting, New Orleans,Nov. 29-30, 1993.

Howe, R. D., Peine, W. J., Kontarinis, D. A., and Son, J. S., "Remote palpation technology," *IEEE Engineering in Medicine and Biology*, **14**(3), pp. 318-323, May/June 1995.

Kontarinis, D. A., Son, J. S., Peine, W. J., and Howe, R. D., "A tactile sensing and display system for teleoperated manipulation," *Proceedings of the 1995 IEEE International Conference on Robotics and Automation*, Nagoya, Japan, pp. 641-646, May 1995.

Lederman, S. J., ""Improving one's touch"...and more," *Perception and Psychophisics*, **24**(2), pp. 154-160, 1978.

Pennypacker, H. S. and Iwata, M. M., "MammaCare: A Case History in Behavioral Medicine," in D. E. Blackman and H. Lejeune, Eds., *Behaviour Analysis in Theory and Practice - Contributions and Controversies*, Lawerence Erlbaum Associates Ltd., East Sussex, U. K., pp. 259-288, 1990.

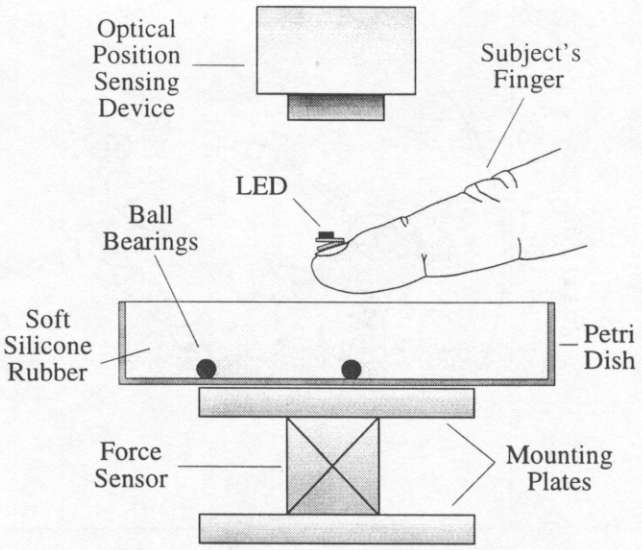

Figure 1. *Experiment Apparatus.* The force sensor measured the normal forces applied to the rubber model and the optical position sensing device, located approximately 70 cm above model, measured the x and y position of the LED (light emitting diode) glued to the subject's fingernail. An opaque screen (not shown) visually isolated the model from the subject.

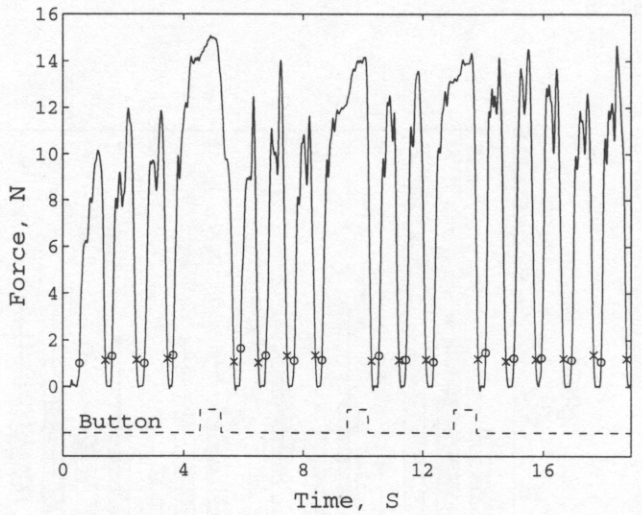

Figure 2. *Force Data from Part of a Typical Trial.* The solid line shows the force data. The dashed line indicates when the subject pushed the button after locating an inclusion. Trials were segmented into a series of individual contact intervals using a threshold of 1 N to find the starting and ending points, shown by O's and X's respectively.

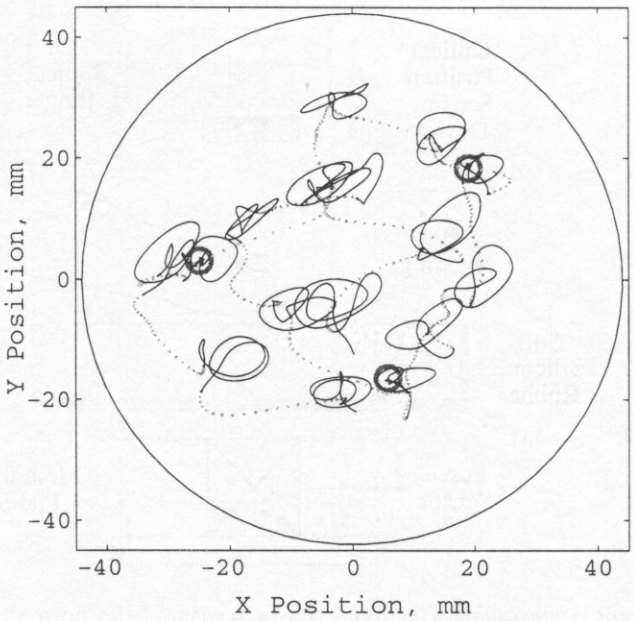

Figure 3. *Segmented x and y Position Data.* (Same Trial Shown in Figure 2.) The solid lines show the path of the finger during the contact intervals. The dotted lines show the path between intervals, when the force was below 1 N, and the three small shaded circles indicate the position and size of the lumps found by the subject. The basic palpation motion used by all of the subjects consisted of pressing into the rubber, making small circles around the initial contact point, retracting out of the rubber, and then moving the finger to a new contact location.

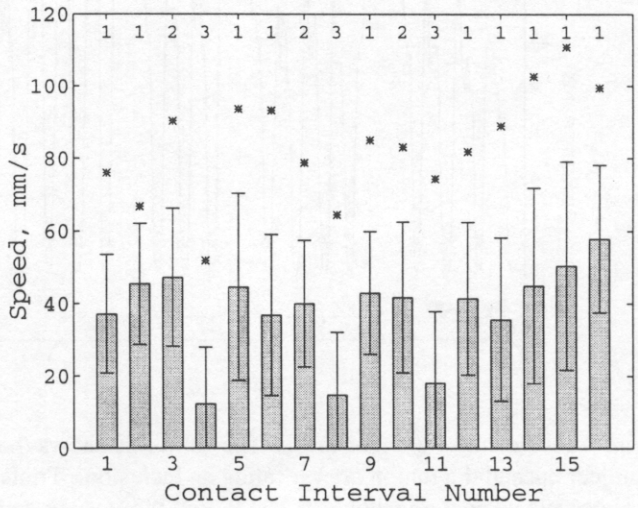

Figure 4. *Finger Speeds During the Typical Trial Shown in Figures 2 and 3.* The height of the bars show the average speed for each contact interval. The error bars indicate the standard deviations, and the asterisks show the maximum speeds during that interval. Numerals at the top indicate contact interval category.

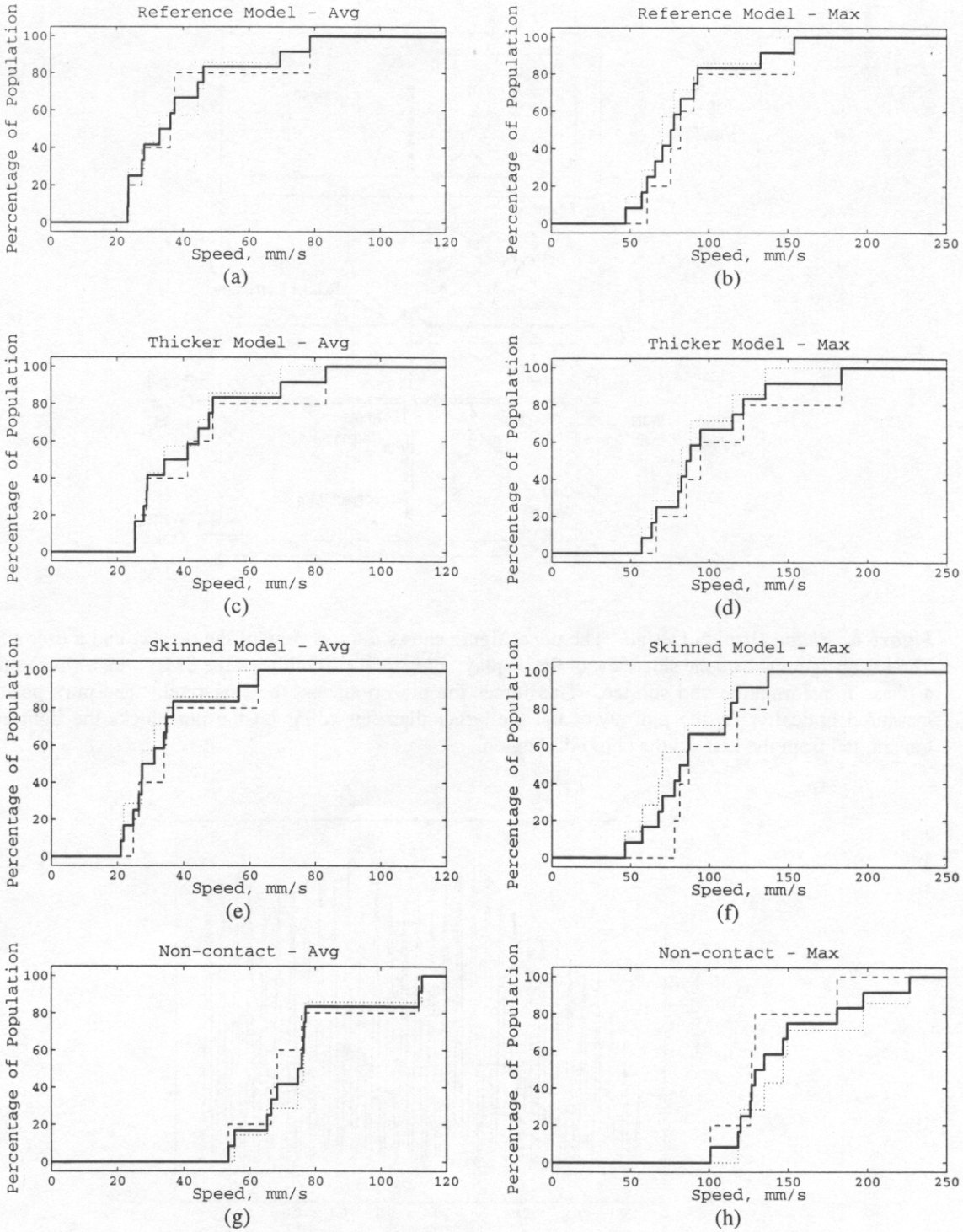

Figure 5. *Cumulative distribution functions for each of the three rubber model types and non-contact case.* The curves indicate the fraction of the population with a mean or average maximum speed below that level. The dashed lines indicate the distribution of experts, the dotted lines indicate the distribution of non-experts, and the solid lines indicate the experts and non-experts combined. Mean and average maximum speeds for (a,b) reference model type, (c,d) thicker model type, (e,f) skinned model type, (g,h) between contact intervals.

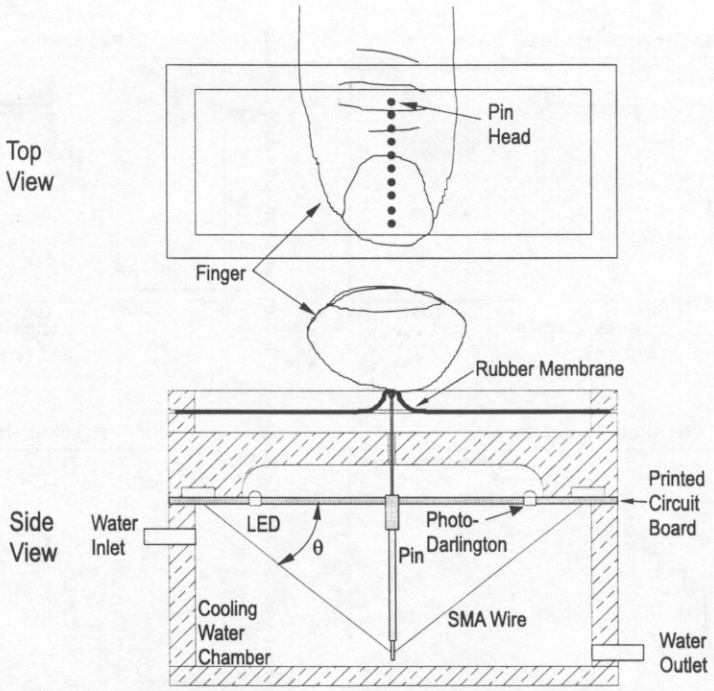

Figure 6. *Shape Display Design.* The upper figure shows the top view of the display and a user's finger. The lower figure shows the side view of the display. Electrical current heats the SMA wires, which undergo a phase transformation and shorten. This forces the pin up against the fingerpad. The pin's position is measured optically. As the pin moves up, the larger diameter collar on the pin blocks the light as it is transmitted from the LED to the photo-darlington.

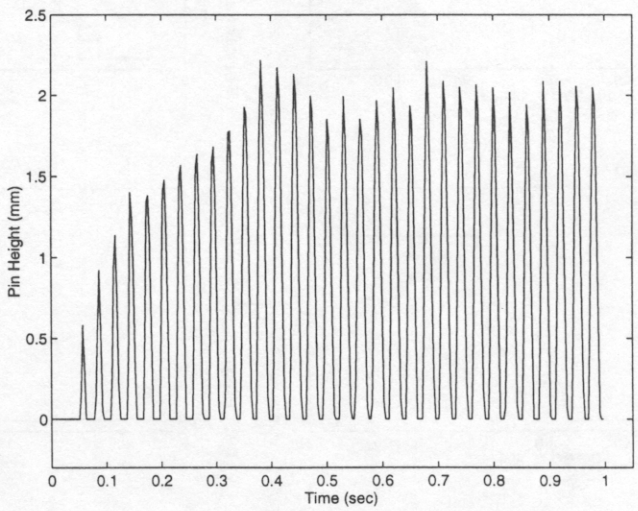

Figure 7. *30 Hz Open Loop Response for One Pin.* The plot shows pin position in response to a 30 Hz triangle wave drive current to the SMA wire. The first few cycles added energy to the wire to heat it up to the transition temperature. The amplitude variations after reaching steady state are due to the variation in cooling flow within the display.